

Wangsa T. Ismaya,<sup>a</sup> Henriëtte J. Rozeboom,<sup>a</sup> Marloes Schurink,<sup>b</sup> Carmen G. Boeriu,<sup>b</sup> Harry Wichers<sup>b</sup> and Bauke W. Dijkstra<sup>a\*</sup>

<sup>a</sup>Laboratory of Biophysical Chemistry, University of Groningen, Nijenborgh 7, 9747 AG Groningen, The Netherlands, and  
<sup>b</sup>Wageningen University and Research Center, PO Box 17, 6700 AA Wageningen, The Netherlands

Correspondence e-mail: b.w.dijkstra@rug.nl

Received 20 December 2010

Accepted 26 February 2011

## Crystallization and preliminary X-ray crystallographic analysis of tyrosinase from the mushroom *Agaricus bisporus*

Tyrosinase catalyzes the conversion of tyrosine to dihydroxyphenylalanine quinone, which is the main precursor for the biosynthesis of melanin. The enzyme from *Agaricus bisporus*, the common button mushroom, was purified and crystallized in two different space groups. Crystals belonging to space group  $P2_1$  (unit-cell parameters  $a = 104.2$ ,  $b = 105.0$ ,  $c = 119.1$  Å,  $\beta = 110.6^\circ$ , four molecules per asymmetric unit) diffracted to 3.0 Å resolution. Crystals belonging to space group  $P2_12_12$  (unit-cell parameters  $a = 104.0$ ,  $b = 104.5$ ,  $c = 108.4$  Å, two molecules per asymmetric unit) diffracted to 2.6 Å resolution. It was essential to include 5 mM  $\text{HoCl}_3$  in all crystallization conditions in order to obtain well diffracting crystals.

### 1. Introduction

Tyrosinase (EC 1.14.18.1) is a copper-containing monooxygenase that is widely distributed in nature, occurring in organisms from all phyla. It catalyzes the *o*-hydroxylation of monophenols (monophenolase activity) and the subsequent oxidation of the *o*-diphenols formed to the corresponding *o*-quinones (diphenolase activity) (Van Gelder *et al.*, 1997), which are precursors for the biosynthesis of melanins. The precise physiological function of the enzyme is not well understood. In mammals, including humans, the enzyme is mainly found in melanocytes, which are pigment-producing cells. The mammalian enzyme has been implicated in pigmentary diseases such as albinism, vitiligo and other melanin-related syndromes (Cesarini, 1996; Hearing, 2005).

In the mushroom *Agaricus bisporus*, tyrosinase has been proposed to be involved in defence mechanisms against pathogens because of the bacteriostatic properties of *o*-quinones and melanins and because of the inducibility of at least one tyrosinase isoform upon microbial challenge (Soler-Rivas *et al.*, 1999). The enzyme is also an important factor in the browning of the mushroom upon aging and microbial infection (Soler-Rivas *et al.*, 1999) and consequently there is substantial interest in its catalytic properties (Espin, Varon *et al.*, 2000; Fenoll *et al.*, 2002; Sánchez-Ferrer *et al.*, 1995) and its inhibition (Kubo *et al.*, 2000; Ley & Bertram, 2001; Zhang *et al.*, 2006).

To date, four genes coding for *A. bisporus* tyrosinase have been described. These genes, *Abppo1* (UniProt protein-sequence database entry Q00024) and *Abppo2* (O42713) (Wichers *et al.*, 2003), and *Abppo3* (C7FF04) and *Abppo4* (C7FF05) (Wu *et al.*, 2010), code for proteins with a molecular mass of 64–67 kDa. However, isolation of the enzyme directly from mushroom fruit bodies yields a heterotetramer composed of two subunits of 43–48 kDa (H chain) and two subunits of 13–14 kDa (L chain) ( $\text{H}_2\text{L}_2$  configuration; Strothkamp *et al.*, 1976). This information led to the hypothesis that tyrosinase is initially formed as a monomeric 64 kDa latent precursor which can be proteolytically activated, resulting in ~43 kDa active forms (Espin, Soler-Rivas *et al.*, 2000). The nature of the L chain is not known. Although the L chain may represent the C-terminal fragment resulting from proteolytic cleavage of the latent precursor, it may also be an unrelated protein that is copurified with active tyrosinase and that is difficult to remove (Flurkey & Inlow, 2008).

X-ray absorption studies have indicated that *A. bisporus* tyrosinase contains two copper ions in its active site with spectroscopic properties resembling those of the two copper ions found in molluscan



haemocyanin, a copper-containing oxygen-carrier protein (Della Longa *et al.*, 1996). The presence of two copper ions in tyrosinase has also been shown in the crystal structure of *Streptomyces castaneoglobisporus* tyrosinase (Matoba *et al.*, 2006), with each of the two copper ions being coordinated by three histidine side chains. However, in *A. bisporus* tyrosinase the side chain of one of these copper-coordinating histidine residues is covalently linked *via* a thioether bond to the side chain of the preceding cysteine residue in the C-X-H sequence motif (Van Gelder *et al.*, 1997). The role of this thioether bond remains elusive. Here, we report the purification and crystallization of commercially available mushroom tyrosinase and preliminary X-ray diffraction data analysis as an initial step towards the elucidation of the three-dimensional structure of the enzyme.

## 2. Materials and methods

### 2.1. Sample preparation

Mushroom tyrosinase powder was purchased from Sigma (Sigma-Aldrich, catalogue No. T3824-250KU) and was purified at 277 K essentially as described previously (Schurink *et al.*, 2007). The mushroom tyrosinase powder was dissolved in 50 mM sodium phosphate buffer pH 6.5 to a concentration of 10 mg ml<sup>-1</sup>. Insoluble material was removed by centrifugation at 277 K and 12 000g for 15 min. The supernatant was carefully recovered and was loaded onto a 10/30 Superdex S-200 column (Amersham Biosciences) equilibrated with 100 mM HEPES buffer pH 7.5 containing 10 mM calcium chloride. Elution from the gel-filtration column was carried out with the same buffer at a constant flow rate of 0.25 ml min<sup>-1</sup>. Fractions with tyrosinase activity were pooled and concentrated with concomitant buffer exchange to 10 mM HEPES pH 7.5 over a 10 kDa cutoff Amicon membrane (Millipore) to a final protein concentration of approximately 6 mg ml<sup>-1</sup>. The concentrated protein was either directly subjected to crystallization experiments or frozen at 253 K for storage.

### 2.2. Determination of protein concentration and enzyme activity

The protein concentration was estimated from the absorption at 280 nm using the experimentally determined  $\epsilon$  value of 132 000 M<sup>-1</sup> cm<sup>-1</sup>. Absorbance measurements were performed with a Nanodrop ND-1000 spectrometer (Nanodrop Technologies Inc., Wilmington, USA).

Enzyme activity was measured at 298 K by a colorimetric method essentially as described previously (Espin *et al.*, 1997) using 3,4-dihydroxyphenylalanine (L-DOPA) as substrate. One unit of tyrosinase activity is defined as the formation of 1  $\mu$ mol L-DOPA quinone per minute. Briefly, in a 1 ml cuvette, 100  $\mu$ l of a 5 mM 3-methyl-2-benzothiazolinone hydrazone (MBTH) solution in water was mixed with 800  $\mu$ l L-DOPA solution (18 mM in 50 mM sodium phosphate buffer pH 6.5). The reaction was started by the addition of 100  $\mu$ l enzyme solution to the reaction mixture. The increase in the absorbance at 484 nm was followed during the first 3 min. The measurements were carried out in an Ultrospec 4300 Pro spectrometer equipped with a temperature-control unit (Amersham Biosciences) interfaced online to a computer. The spectra were recorded and processed with the time-drive measurement module (*SWIFT II* program, v.2.01, Amersham Biosciences).

### 2.3. Characterization of protein samples

The purity of the enzyme was routinely checked by SDS-PAGE using a PhastGel System (Amersham Biosciences) with pre-cast SDS

gels and electrode strips. Staining was conducted in the same system using silver nitrate as the staining solution.

The temperature-stability of the protein in solution was analyzed by thermal shift assay (Ericsson *et al.*, 2006). Briefly, 5  $\mu$ l 200-fold diluted SYPRO Orange solution (Invitrogen, Breda, The Netherlands) as a molecular probe, 5  $\mu$ l 4.5 mg ml<sup>-1</sup> enzyme solution in water, 2.5  $\mu$ l 1 M buffer stock solution and 2.5–5  $\mu$ l additive stock solution were mixed in a 96-well thin-wall PCR plate (Bio-Rad). The final reaction volume was adjusted to 25  $\mu$ l by adding an appropriate volume of filtered and degassed Milli-Q water. The plate was sealed with optical quality sealing tape (Bio-Rad Laboratories BV, Veenendaal, The Netherlands). The sealed plate was inserted into a real-time PCR machine (iCycler, Bio-Rad Laboratories BV, Veenendaal, The Netherlands) and was heated from 293 to 363 K with a 0.5 K increment per 20 s. The changes in fluorescence of the SYPRO Orange probe were monitored with a fluorescence detector (MyIQ single-colour RT-PCR detection system, Bio-Rad) at excitation and emission wavelengths of 490 and 575 nm, respectively.

The monodispersity of the enzyme was analyzed by dynamic light scattering using a DynaPro dynamic light-scattering instrument (Wyatt Technologies, Santa Barbara, USA). The protein sample (1 mg ml<sup>-1</sup>) was centrifuged at 12 000g for 15 min at 277 K and the supernatant was carefully transferred into a DLS cuvette. Measurements were performed at both 298 and 277 K.

### 2.4. Crystallization procedures

Initial screening for crystallization conditions was carried out at 298 K by the sitting-drop vapour-diffusion method employing an Oryx-6 crystallization robot (Douglas Instruments, Hungerford, England) equipped with an anti-evaporation shielding plate. The following commercial screens were used in 96-well CrystalClear strips for sitting-drop setups (Hampton Research): Structure Screens I and II (Molecular Dimensions, Apopka, USA), Cryoscreens I and II (Emerald BioSystems, Bainbridge Island, USA) and the JCSG+ Suite (Qiagen, Venlo, The Netherlands). The starting volume of the drop was 0.3  $\mu$ l, consisting of 0.12  $\mu$ l protein solution and 0.18  $\mu$ l reservoir solution. Optimization of promising crystallization conditions was performed with the hanging-drop vapour-diffusion method, varying the precipitant type and concentration, the temperature and the pH and using additives.

### 2.5. Data collection and processing

Prior to X-ray diffraction analysis, crystals were transferred into a cryoprotectant solution consisting of 15% PEG 4000, 20% PEG 400, 1 mM HoCl<sub>3</sub> and 100 mM sodium acetate buffer pH 4.6 before flash-freezing them in liquid nitrogen. X-ray diffraction experiments were carried out on beamlines BM16, ID23-2 and ID14-4 at the ESRF (Grenoble, France). Diffraction data were recorded at 100 K with the CCD detector available at the beamline with 0.5–1.0° oscillations. The data sets were processed using either *XDS* (Kabsch, 2010) or *MOSFLM* (Leslie, 2006). Scaling and merging were performed with *SCALA* (Evans, 2006), which is part of the *CCP4* program suite (Collaborative Computational Project, Number 4, 1994).

## 3. Results and discussion

Commercially available mushroom tyrosinase was successfully purified using a single gel-filtration step. In the elution profile, tyrosinase activity was detected in a peak with a retention time corresponding to a molecular mass of ~120 kDa, as expected for the mass of the H<sub>2</sub>L<sub>2</sub> form of mushroom tyrosinase (Strothkamp *et al.*, 1976). Furthermore,

SDS-PAGE analysis of this peak confirmed the presence of the heavy (H) and light (L) chains, with molecular weights of 45 and 14 kDa, respectively, which is in agreement with previous reports (Schurink *et al.*, 2007). Analysis of the protein content and specific activity indicated that approximately 50% of the total protein in the mushroom tyrosinase powder consisted of tyrosinase. The purification scheme recovered up to 90% of the enzyme activity.

The thermostability of tyrosinase was investigated by following the unfolding of the protein as a function of temperature under various conditions (Ericsson *et al.*, 2006). A shift in the melting temperature ( $T_m$ ) of the protein to higher values indicates an increase in thermostability. Fig. 1(a) shows that the enzyme demonstrated the highest  $T_m$  value in 100 mM HEPES buffer pH 7.5, 10 mM CaCl<sub>2</sub>. In the absence of calcium or when the calcium was replaced by sodium the  $T_m$  value shifted to lower temperatures. Based on this observation, 100 mM HEPES buffer pH 7.5 with 10 mM CaCl<sub>2</sub> was chosen for the purification.

To assess the aggregation behaviour of tyrosinase, a dynamic light-scattering experiment was performed. Without applying any noise reduction or peak filtering, the fit on mass showed one main peak with a mean  $R_h$  of 4.4 nm and 6% polydispersity, indicating a monodisperse solution at 298 K (Fig. 1b). The calculated mass of this peak was 110 kDa, which is in agreement with the results of size-

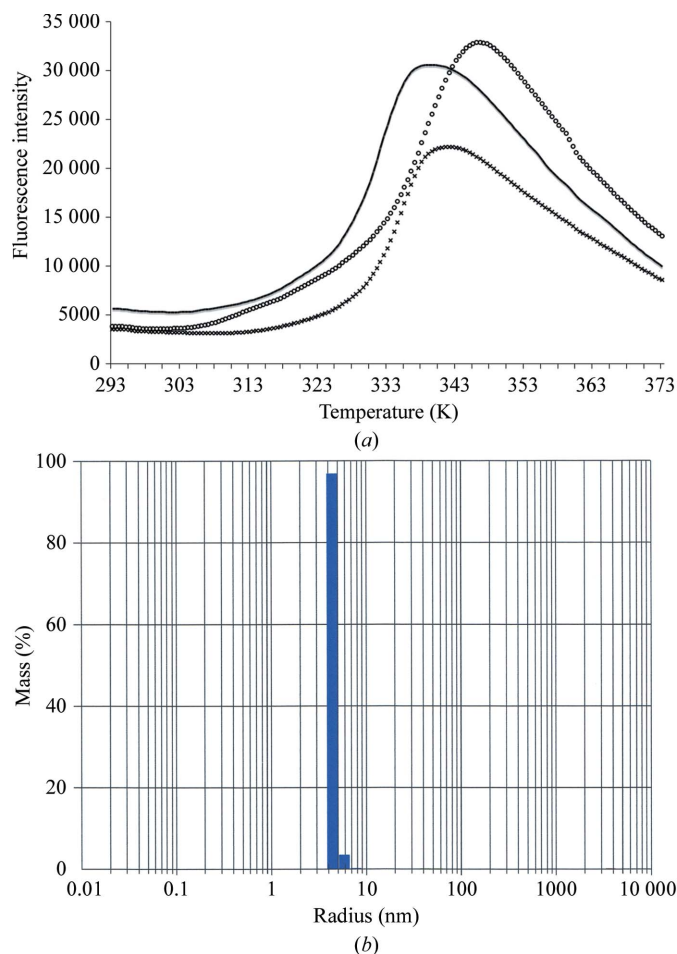


**Figure 1**  
Stability and monodispersity of tyrosinase in solution. (a) Thermal unfolding of tyrosinase in 100 mM HEPES buffer pH 7.5 (black line), in 100 mM HEPES buffer with an additional 10 mM calcium chloride (circles) or in 100 mM HEPES buffer with an additional 10 mM sodium chloride (crosses). (b) Monodispersity of tyrosinase in 100 mM HEPES buffer pH 7.5 containing 10 mM CaCl<sub>2</sub> at 298 K.

**Table 1**  
Summary of crystallographic data collection and processing.

Values in parentheses are for the highest resolution shell.

	Native $P2_1$	Native $P2_12_12$
Beamline	ESRF ID23-2	ESRF ID14-4
Wavelength (Å)	0.8726	0.9395
Resolution (Å)	50.0–3.00	54.2–2.60
Unit-cell parameters (Å, °)	$a = 104.2, b = 105.0,$ $c = 119.1, \beta = 110.6$	$a = 104.0, b = 104.5,$ $c = 108.4, \beta = 90$
$R_{\text{merge}}^\dagger$	0.16 (0.34)	0.12 (0.45)
$R_{\text{p.i.m.}}^\ddagger$	0.11 (0.24)	0.07 (0.28)
Mean $I/\sigma(I)$	7.3 (2.3)	8.2 (2.3)
Completeness (%)	88.9 (90.5)	94.8 (81.8)
Multiplicity	2.8 (2.9)	4.0 (2.7)

$^\dagger R_{\text{merge}} = \frac{\sum_{hkl} \sum_i |I_i(hkl) - \langle I(hkl) \rangle|}{\sum_{hkl} \sum_i I_i(hkl)}$ ;  $R_{\text{p.i.m.}} = \frac{\sum_{hkl} [1/(N-1)]^{1/2} \times \sum_i |I_i(hkl) - \langle I(hkl) \rangle|}{\sum_{hkl} \sum_i I_i(hkl)}$ , where  $I_i(hkl)$  is the integrated intensity of a reflection,  $\langle I(hkl) \rangle$  is the mean intensity of multiple corresponding symmetry-related reflections and  $N$  is the multiplicity of the given reflections.

exclusion chromatography, and confirmed the presence of an H<sub>2</sub>L<sub>2</sub> tetramer in solution (Strothkamp *et al.*, 1976). Although some noise was observed owing to protein aggregation, it resulted from less than 0.1% of the mass in the sample. Because the monodispersity of the enzyme solution was reduced at 277 K (data not shown), subsequent crystallization experiments were carried out at 298 K.

Initial crystals were obtained with the JCSG+ screen after 48 h at 298 K using a reservoir solution composed of 8% PEG 4000 in 100 mM sodium acetate buffer pH 4.6. However, these crystals only diffracted to  $\sim 8$  Å resolution (BM16, ESRF, Grenoble). Optimization using the hanging-drop vapour-diffusion method, followed by an extensive additive screen, revealed that 5 mM HoCl<sub>3</sub> improved the diffraction quality of the crystals. After this discovery, plate-shaped crystals suitable for X-ray data collection (Fig. 2) were routinely obtained from drops consisting of 2  $\mu$ l protein solution ( $\sim 6$  mg ml<sup>-1</sup>) and 2  $\mu$ l reservoir solution, which were suspended over 800  $\mu$ l reservoir solution consisting of 10% (w/v) PEG 4000, 100 mM sodium acetate buffer pH 4.6 and 5 mM HoCl<sub>3</sub>. Crystals with reasonable size (200  $\times$  200  $\times$  50  $\mu$ m) could be obtained within 4–5 d. They diffracted to 2.6 Å resolution using synchrotron radiation (ESRF, Grenoble). Finally, it appeared to be necessary to include 1 mM HoCl<sub>3</sub> in the cryoprotectant solution for reproducible diffraction by the crystals.

The crystals obtained were analyzed by X-ray diffraction (Table 1). They belonged to either space group  $P2_1$  or space group  $P2_12_12$ . Crystals with space group  $P2_1$  had unit-cell parameters  $a = 104.2, b = 105.0, c = 119.1$  Å,  $\beta = 110.6^\circ$  and diffracted to 3.0 Å resolution.

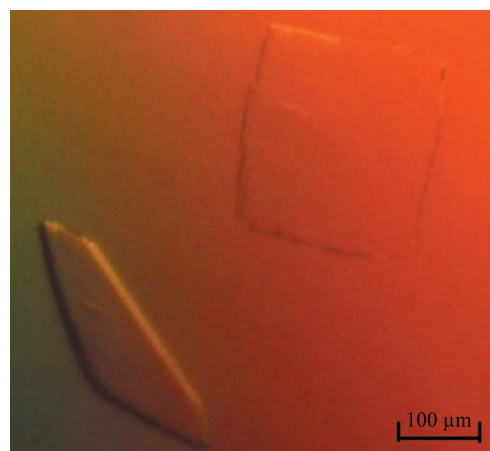


**Figure 2**  
Plate-shaped crystals of mushroom tyrosinase.

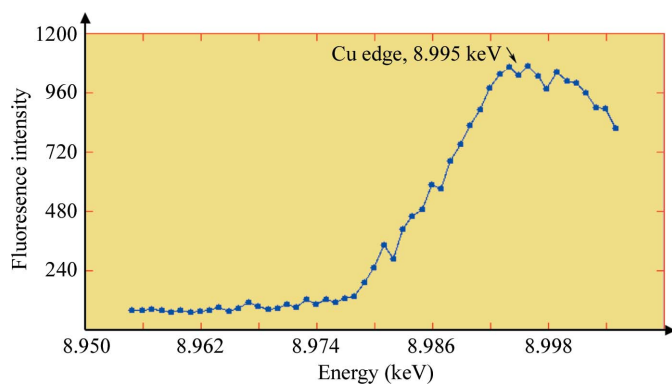


**Figure 3**  
Energy scan of a tyrosinase crystal. The peak occurs at an energy of  $\sim 8.995 \pm 0.001$  keV, which is specific for copper in tyrosinase (Della Longa *et al.*, 1996).

Crystals with space group  $P2_12_12$  had unit-cell parameters  $a = 104.0$ ,  $b = 104.5$ ,  $c = 108.4$  Å and diffracted to 2.6 Å resolution. Assuming the presence of four 60 kDa HL heterodimers per asymmetric unit in the  $P2_1$  crystals and two HL heterodimers per asymmetric unit in the  $P2_12_12$  crystals gave similar values for the Matthews coefficient and solvent content of  $\sim 2.4$  Å<sup>3</sup> Da<sup>-1</sup> and 49%, respectively. Data-collection statistics are summarized in Table 1.

An SDS-PAGE analysis of a tyrosinase crystal showed the presence of both the 45 and 14 kDa polypeptides, indicating that both the H and L chains are present in the crystal. Furthermore, an X-ray fluorescence scan of a tyrosinase crystal grown in the absence of  $\text{HoCl}_3$  showed the presence of copper in the protein crystal (Fig. 3). Finally, significant tyrosinase activity was observed after dissolving a crystal that had been exposed to X-rays. Since the activity of the enzyme relies on the presence of the copper in the active site, this result not only confirmed the presence of copper but also indicates that the copper is still functional. Thus, we have crystallized active mushroom tyrosinase. We are currently trying to solve the structure of the enzyme by molecular replacement with multiple-crystal averaging using as search models the structures of the core domain of *Octopus dofleini* haemocyanin (PDB entry 1js8; Cuff *et al.*, 1998) and *S. castaneoglobisporus* tyrosinase (PDB entry 1wx2; Matoba *et al.*, 2006), which have sequence identities of 19% and 20% for 274 and 275 aligned amino acids, respectively.

We thank the beamline scientists at BM16, ID23-2 and ID14-4 (ESRF, Grenoble, France) for their support during data collection.

This work was funded by the Innovation-driven Research Program for Industrial Proteins (project No. IIE00022). Data collection at the ESRF was supported by the ESRF and by the European Molecular Biology Laboratory (EMBL) under the European Community's Seventh Framework Program (FP7/2007–2013, grant agreement No. 226716).

## References

- Cesarini, J. P. (1996). *Adv. Space Res.* **18**, 35–40.  
Collaborative Computational Project, Number 4 (1994). *Acta Cryst.* **D50**, 760–763.  
Cuff, M. E., Miller, K. I., van Holde, K. E. & Hendrickson, W. A. (1998). *J. Mol. Biol.* **278**, 855–870.  
Della Longa, S., Ascone, I., Bianconi, A., Bonfigli, A., Castellano, A. C., Zarivi, O. & Miranda, M. (1996). *J. Biol. Chem.* **271**, 21025–21030.  
Ericsson, U. B., Hallberg, B. M., Detitta, G. T., Dekker, N. & Nordlund, P. (2006). *Anal. Biochem.* **357**, 289–298.  
Espin, J. C., Morales, M., Garcia-Ruiz, P. A., Tudela, J. & Garcia-Canovas, F. (1997). *J. Agric. Food Chem.* **45**, 1084–1090.  
Espin, J. C., Soler-Rivas, C. & Wichers, H. J. (2000). *Mushroom Sci.* **15**, 79–86.  
Espin, J. C., Varon, R., Fenoll, L. G., Gilabert, M. A., Garcia-Ruiz, P. A., Tudela, J. & Garcia-Canovas, F. (2000). *Eur. J. Biochem.* **267**, 1270–1279.  
Evans, P. (2006). *Acta Cryst.* **D62**, 72–82.  
Fenoll, L. G., Rodríguez-López, J. N., García-Molina, F., García-Cánovas, F. & Tudela, J. (2002). *IUBMB Life*, **54**, 137–141.  
Flurkey, W. H. & Inlow, J. K. (2008). *J. Inorg. Biochem.* **102**, 2160–2170.  
Gelder, C. W. van, Flurkey, W. H. & Wichers, H. J. (1997). *Phytochemistry*, **45**, 1309–1323.  
Hearing, V. J. (2005). *J. Dermatol. Sci.* **37**, 3–14.  
Kabsch, W. (2010). *Acta Cryst.* **D66**, 125–132.  
Kubo, I., Kinst-Hori, I., Kubo, Y., Yamagiwa, Y., Kamikawa, T. & Haraguchi, H. (2000). *J. Agric. Food Chem.* **48**, 1393–1399.  
Leslie, A. G. W. (2006). *Acta Cryst.* **D62**, 48–57.  
Ley, J. P. & Bertram, H. J. (2001). *Bioorg. Med. Chem.* **9**, 1879–1885.  
Matoba, Y., Kumagai, T., Yamamoto, A., Yoshitsu, H. & Sugiyama, M. (2006). *J. Biol. Chem.* **281**, 8981–8990.  
Sánchez-Ferrer, A., Rodríguez-López, J. N., García-Cánovas, F. & García-Carmona, F. (1995). *Biochim. Biophys. Acta*, **1247**, 1–11.  
Schurink, M., van Berkel, W. J., Wichers, H. J. & Boeriu, C. G. (2007). *Peptides*, **28**, 485–495.  
Soler-Rivas, C., Jolivet, S., Arpin, N., Olivier, J. M. & Wichers, H. J. (1999). *FEMS Microbiol. Rev.* **23**, 591–614.  
Strothkamp, K. G., Jolley, R. L. & Mason, H. S. (1976). *Biochem. Biophys. Res. Commun.* **70**, 519–524.  
Wichers, H. J., Recourt, K., Hendriks, M., Ebbelaar, C. E. M., Biancone, G., Hoerberichs, F. A., Mooibroek, H. & Soler-Rivas, C. (2003). *Appl. Microbiol. Biotech.* **61**, 336–341.  
Wu, J., Chen, H., Gao, J., Liu, X., Cheng, W. & Ma, X. (2010). *Biotechnol. Lett.* **32**, 1439–1447.  
Zhang, J.-P., Chen, Q.-X., Song, K.-K. & Xie, J.-J. (2006). *Food Chem.* **95**, 579–584.